Sampling Error Variation due to Rainfall Seasonality

Yoo, Chulsang
Associate Prof., Dept. of Envir. Engrg, Korea University, Jochiwon, Korea

ABSTRACT: In this study, we characterized the variation of sampling errors using the Waymire-Gupta-Rodriguez-Iturbe multi-dimensional rainfall model (WGR model). The parameters used for this study are those derived by Jung et al. (2000) for the Han River Basin using a genetic algorithm technique. The sampling error problems considering in this study are those for using raingauge network, satellite observation and also for both combined. The characterization of sampling errors was done for each month and also for the downstream plain area and the upstream mountain area, separately. As results of the study we conclude: (1) The pattern of sampling errors estimated are obviously different from the seasonal pattern of monthly rainfall amounts. This result may be understood from the fact that the sampling error is estimated not simply by considering the rainfall amounts, but by considering all the mechanisms controlling the rainfall propagation along with its generation and decay. As the major mechanism of moisture source to the Korean Peninsula is obviously different each month, it seems rather normal to provide different pattern of sampling errors from that of monthly rainfall amounts. (2) The sampling errors estimated for the upstream mountain area is about twice higher than those for the down stream plain area. It is believed to be because of the higher variability of rainfall in the upstream mountain area than in the down stream plain area.

1 INTRODUCTION

Sampling error is inherent as the rainfall observation cannot be continuous both in time and space. For example, the raingauge measures rainfall continuously in time but discretely in space. On the other hand, radar or satellite observes the rainfall field continuously in space but discretely in time. This inherent gab causes some errors in estimating the area-time average of rainfall depth.

Basically the sampling error can be estimated using the rainfall measurements conditioning that they are three-dimensional in time and space. However, this kind of data is generally unavailable, so we follow a rather indirect way using a multi-dimensional rainfall model. A multi-dimensional model of rainfall counts all observed characteristics of rainfall both in physical and statistical point of view. This kind of multi-dimensional rainfall models can be helpful not only to characterize the rainfall field, but also to make various application studies easy as in many cases their structures are available analytically (North and Nakamoto, 1989; North et al., 1994; Ha and North, 1994; Valdes et al., 1994). So far, many multi-dimensional rainfall models have been developed for various purposes, like realistic rainfall simulation, sampling strategy, and calibration of sensors. Examples are the Waymire-Gupta-Rodriguez-Iturbe multi-dimensional rainfall model (Waymire, Gupta, and Rodriguez-Iturbe, 1984; hereafter the WGR model), the noise forced diffusive model (North and Nakamoto, 1989), and recently a model by Yoo et al. (1996). Each model has its own advantages and disadvantages in practical use. A complex model, like the WGR model, can represent the rainfall field more accurately provided the proper estimates of parameters are used. However, as shown by Islam et al. (1988), Valdes et al. (1990) and Koepsell and Valdes (1991), its parameter estimation has been a difficult task. A relatively simple model, like the noise forced diffusive rainfall model, has advantages of easy parameter estimation and application to the other purposes (mainly due to the simple model structure with a small set of parameters), but it lacks proper description of physical and statistical features of observed rainfall fields (Valdes et al., 1994). The model by Yoo et al. (1996) may be said to be in between the above two. It has relatively simple form with only four parameters. Its parameter estimation is also simple, but it lacks the description of long-term storm arrival system and spatial clustering.

The sampling error to be estimated in this study is for analyzing its variation due to the seasonal variation of rainfall amounts. As we well aware, the rainfall seasonality is quite common in the Monsoon area. So far, there have been many cases to estimate the sampling errors for a specific season of a region (North and Nakamoto, 1989; Graves et al., 1993), but no attempts have been made to evaluate the sampling error variation due to the rainfall seasonality.

In this study, we are to use the WGR model for the sampling error study. Even though the structure of the

WGR model is very complex and non-linear, we believe this model is the best one we can choose for the study purpose. Basically, the characterization of rainfall fields using the WGR model is done by its parameter estimation, generally using the first- and second-order statistics numerically derived from point gauge measurements. Recently, Jung et al. (2000) estimated the WGR model parameters for the Han River Basin using a genetic algorithm technique and showed their validity by comparing the model statistics with those observed. As the parameters estimated are for several cases of seasonal and regional rainfalls, we may be easily apply them to characterize the sampling characteristics for various cases. The sampling error problems considering in this study are for raingauge network, the satellite observation, and for the combined cases. By comparing the sampling errors estimated, we will quantify the variation of sampling errors due to the rainfall seasonality.

2 THE WGR MODEL AND ITS PARAMETER ESTIMATION

2.1 Model Description

The WGR model (Waymire et al., 1984) was developed to represent meso-scale (about 20-200km) rainfall. As a conceptual model, this model shows a good link between atmospheric dynamics and a statistical description of meso-scale rainfall. The model represents rainfall in a hierarchical approach with rain cells embedded in cluster potential centers, which are in turn embedded in rainbands. The Poisson process was introduced for the rainbands arrival scheme and the spatial Poisson process to distribute the cluster potentials within a rainband. The occurrences of rain cells within the cluster potentials and the rainband following are assumed to be a random number of points independently and identically distributed in the space-time cylinder with common probability density function.

The representation of the ground-level rainfall intensity (at location x and time t) of the model can be written as follows

$$\xi(t,x) = \int_{-\infty}^{t}\int_{R^d} g[t-s,|x-y-v(t-s)|]X(s,y)dsdy$$
$$= \int_{-\infty}^{t} g_1(t-s)Z[s,x-v(t-s)]ds \quad (1)$$

where, v is a uniform and steady drift velocity vector and $Z(t, x)$ is given by

$$Z(t,x) = \int_{R^2} g_2(x-y)X(t,y)dy \quad (2)$$

where the two-stage point cluster field $X(t,y)$, a random field, governs the instantaneous generation of rain cells in time and space, and the kernel $g_2(r)$ distributes the rainfall intensity in space around each cell. The kernel $g_1(t)$ represents the temporal evolution of the life cycle of a rain cell. Table 1 shows typical parameters and their descriptions. More description of the model can be found in Waymire et al. (1984) and Gupta and Waymire (1987).

The analytical form of the frequency-wavenumber spectrum of the WGR model was derived by Valdes et al (1990);

$$S(f,\nu_x,\nu_y) = \theta_1\frac{\alpha E(D,0)}{\alpha^2+\Theta^2} + \theta_2\frac{2\alpha\beta(\beta^2-\alpha^2)}{(\alpha^2+4\pi^2f^2)(\beta^2+4\pi^2f^2)}\delta(\nu_x)\delta(\nu_y)$$
$$+\theta_3\frac{\alpha\beta(\beta^2-\alpha^2)}{(\alpha^2+\Theta^2)(\beta^2+\Theta^2)}\frac{E(D,\sigma)}{4\pi^2(D^2+\sigma^2)} \quad (3)$$

where, $\delta()$ is a *dirac delta function* and:

$$E(D,\sigma) = 8\pi(D^2+\sigma^2)\exp\{-4\pi^2(D^2+\sigma^2)(\nu_x^2+\nu_y^2)\}$$
$$\Theta = 2\pi(\nu_x U_x + \nu_y U_y + f)$$

This spectrum shows the dependencies of order -2 and -4 on both frequency and wavenumber. These dependencies are the consequence of the exponential descriptions of rainfall intensity decay in time and the Gaussian kernel to distribute the rainfall intensity in space (Yoo et al, 1996).

2.2 Model Non-linearity and Parameter Estimation

The extreme difficulties associated with the estimation of the WGR model parameters are recognized to be a major impediment to its wider use and full utilization. It is mainly because of the fact that most of the WGR

model parameters are not physically measurable.

The WGR model has nine parameters: λ_m, α, β, $E[i_0]$, $E[v]$, ρ_l, D, σ and U, which may be evaluated using the method of moments. Various combinations of first- and second-order statistics from historical rainfall data can be equated to their theoretical expressions, resulting in a set of nine highly nonlinear equations with nine unknowns. However, although theoretically possible, it appears unrealistic to attempt to solve nine simultaneous equations (Islam et al., 1988; Valdes et al., 1990; Koepsell and Valdes, 1991). Rather, it is recommended to use a combination of physically determined parameters and parameters estimated from data. Generally three parameters, D, σ and U, are determined from physical consideration and kept fixed while other six were estimated using the method of moments (Islam et al., 1988).

This results in a set of six equations with six unknown parameters. A minimum least square technique has been employed to obtain estimates of the model parameters. Let $F(X)$ be the set of nonlinear equations in parameter X that must satisfy the observation vector θ:

$$F(\hat{X}) - \theta = 0 \tag{4}$$

where $F(\hat{X})$ is the best estimate of θ. The elements in θ have different order of magnitudes and hence their sum of the squares tend to be biased toward higher values. To circumvent this problem, every $F(X)$ is normalized by the corresponding θ value. Now, the solution of (4) may be derived through a simple unconstrained nonlinear minimization:

$$\min X\{(\frac{f_1(X)}{\theta_1}-1)^2+(\frac{f_2(X)}{\theta_{21}}-1)^2+\Lambda+(\frac{f_t(X)}{\theta_t}-1)^2+\Lambda\} \tag{5}$$

In this study we used the parameters estimated by Jung et al. (2000) for further analysis. Their estimation procedure also utilized a combination of physically determined parameters and parameters to be estimated from the data. The parameters, D and σ are chosen to be 1.6~2.6 km and 7~9 km, respectively, from the observation of radar snapshots. The cell velocity U was determined from the climatological conditions for each month, which was set to be 7 to 11 km/hour (Korea Meteorological Administration, 1995).

The other parameters estimated are summarized in Table 2 for the downstream plain area and the upstream mountain area, respectively. Also, Tables 3 and 4 compares the observed and model statistics for the cases we consider. From these tables we can easily find the rainfall seasonality captured in the WGR model parameters. Basically, the high rainfall amount in the rainy season can be explained by the arrival rate of rain bands, mean number of cells per cluster potential center, and raincell intensity. When also comparing the parameters estimated for the downstream plain area and upstream mountain area, an obvious distinction can be found in the number of storms. That is, the number of storms in the mountain area was estimated to be significantly higher than that in the plain area. Thus, due to the orographic effect, more frequent storms can be expected to happen in the mountain area, but, still, the total amount of rainfall in a given period seems to remain almost the same as in the downstream plain area. It is because the cell intensity estimated for the upstream mountain area is a bit less than that for the downstream plain area. This difference is also believed to affect on the sampling error variation as well as the rainfall seasonality. More in detail description of the WGR model parameter estimation can be found in Jung et al. (2000).

3 VARIATION OF SAMPLING ERRORS DUE TO RAINFALL SEASONALITY

North and Nakamoto (1989) derived a formalism for calculating the sampling errors from satellites or raingauge networks (see also Yoo (2000)). Their equation for sampling error contains three integrals both in wavenumber and frequency domains for design filter and rainfall spectrum. The design filter is dependent on the sampling design such as field size, sampling duration, sampling interval, distance between raingauges, etc. Thus, with given setting of sampling design one can calculate the sampling error, or he can also design a sampling plan for raingauge network, satellite visit schedule, or both combined with the maximum tolerable sampling error given. The equation for sampling error is given as,

$$\varepsilon^2 = \sigma^2 \iiint |H(v_x, v_y, f)|^2 S(v_x, v_y, f) dv_x dv_y df \tag{6}$$

where, $|H|^2$ is the design filter, S is the rainfall spectrum, and σ^2 is the variance of the continuous rainfall field.

For the case of raingauge network design, equally spaced both in x- and y-direction by Δx and Δy

over $L_1 \times L_2$ domain, the design filter is expressed such as

$$|H|^2 = G^2(\pi v_x L_1) G^2(\pi v_y L_2) G^2(\pi f T) \left[1 - \frac{1}{G(\pi v_x \Delta x) G(\pi v_y \Delta y)} \right]^2 \tag{7}$$

where, $G(x)=sin\ (x)/x$ is the Bartlett filter. As the Bartlett filter, $G(x)$, converges to one when x approaches zero, if the dimension L of the averaging area vanishes, the above formalism will predict the expected point results. The design filter for the satellite observation every Δt during the period of T can also be expressed as:

$$|H|^2 = G^2(\pi v_x L_1) G^2(\pi v_y L_2) G^2(\pi f T) \left[1 - \frac{1}{G(\pi f \Delta t)} \right]^2 \tag{8}$$

where, $L_1 \times L_2 = A$ is the spatial scale for satellite observation.

The analytical form of the sampling error from satellite observations for the WGR model was derived by Graves et al. (1993), which is

$$\varepsilon_s^2 = \frac{1}{L^2 T} < \frac{8\pi\theta_1 D^2}{\alpha} \{ \frac{\alpha \Delta t}{2} \coth(\frac{\alpha \Delta t}{2}) - 1 \}]$$
$$+ 2(\theta_2 L^2 + \theta_3)[\frac{\Delta t}{2} \{ \beta \coth(\frac{\alpha \Delta t}{2}) - \alpha \coth(\frac{\beta \Delta t}{2}) \} + \frac{\alpha^2 - \alpha^2}{\alpha\beta}] > \tag{9}$$

Graves et al. (1993) also derived the equation for the sampling error from raingauge networks for the WGR model, which is

$$\varepsilon_s^2 = \frac{4}{L^2 T} < \frac{8\pi\theta_1 D^2 \alpha}{\alpha} \sum_{n,m=1}^{\infty} \frac{\exp[-4\pi^2 D^2 (n^2 + m^2)/\Delta l^2]}{[\alpha^2 + 4\pi^2 \Theta]/\Delta l^2]}$$
$$+ 2\theta_3 \alpha\beta(\beta^2 - \alpha^2) \sum_{n,m=1}^{\infty} \frac{\exp[-4\pi^2 (D^2 + \sigma^2)(n^2 + m^2)/\Delta l^2]}{[\alpha^2 + 4\pi^2 \Theta^2/\Delta l^2][\beta^2 + 4\pi^2 \Theta^2/\Delta l^2]} > \tag{10}$$

where $\Theta = v_x n + v_y m$. As it is difficult to estimate the variance of the continuous rainfall field, we also had better replace it by the variance of area averaged field, σ_A^2, which can be expressed such as,

$$\sigma_A^2 = \sigma^2 \iiint G^2(\pi v_x L_1) G^2(\pi v_y L_2) S(v_x, v_y, f) dv_x dv_y df \tag{11}$$

Also, for the WGR model, the variance of the area average rainfall can be derived:

$$\sigma_A^2 = \frac{1}{L^2} [4\pi D^2 \theta_1 + (\beta - \alpha)\theta_3] + (\beta - \alpha)\theta_2 \tag{12}$$

Seasonal variation of the sampling errors both from raingauge networks and from satellite observations is investigated by estimating the sampling error using the WGR model with the parameters estimated monthly and also regionally in the previous section. The size of the sampling domain is assumed to be 160km x 160km considering the size of the Han River Basin. Total 56 raingauges are also located evenly over the basin ($\Delta l = 20km$). The revisit interval of satellite observation is assumed to be 12 hours, and total sampling duration for both cases is assumed to be one month (720 hours).

The sampling errors estimated are summarized in Figures 1 and 2 for the mountain area and the plain area, respectively. The sampling error for the whole basin is more or less the same as the arithmetic average of the two. In these figures we also plotted the sampling errors for the combined sampling case using both the raingauge network and the satellite. The sampling errors for the combined sampling case can be easily estimated as a harmonic mean of both from satellite and raingauge network (North et al., 1991; Graves et al., 1993).

As can be seen from Figures 1 and 2, the variation of sampling errors is not so obvious compare to the rainfall seasonality. If not considering the case of October, we may say there exists a slight seasonality of the sampling errors as those for July are a little higher than those for other months. However, the sampling errors estimated for October, then is a dry month, are much higher than those for July, also those for May, also a dry month, are similar to those for July.

The reason of this somewhat unexpected result may be found in the characteristics of rainfall both in time and space. Obviously, the sampling error is estimated not simply by considering the rainfall amounts, but by

considering all the mechanisms controlling the rainfall propagation along with its generation and decay. Thus, the sampling errors estimated differently from the seasonal pattern of monthly rainfall amounts may be understood as results considering different rainfall mechanisms. Quite interestingly, even though there is an obvious seasonality in the monthly rainfall amounts observed in the Korean Peninsula, the major mechanism of moisture source to the Korean Peninsula is obviously different each month.

First, before the beginning of the Monsoon season, which lasted about a month from the end of June, the Korea Peninsula receives only the scattered shower to leave the land in a dry condition. However, after the Monsoon begins, the Korean Peninsula receives large amount of rains generally covering the whole Peninsula along with long rainfall duration, sometimes lasted for several days. And, from the end of July after the Monsoon season has ended, the Korean Peninsular once again receives only the scattered shower but with much higher intensity than that in June. It also lasted almost one month just before the end of August, when the typhoon season begins. More or less ten typhoons have been reached the Korea Peninsula, among which three or four cross the Peninsula. Finally, at the end of September another dry season begins with scattered showers but with much less intensity than that in June.

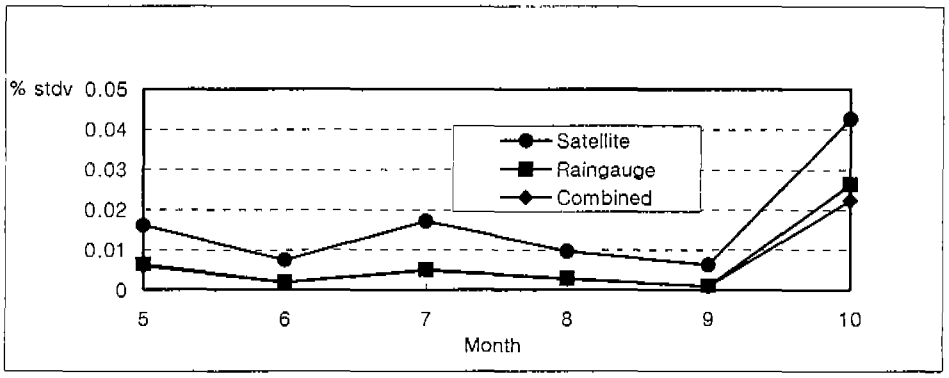

Fig. 1. Sampling error variation in the upstream mountain area

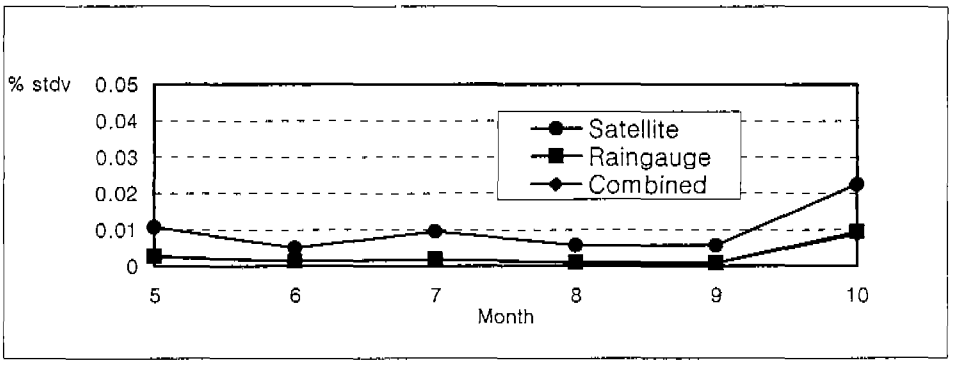

Fig. 1. Sampling error variation in the downstream plain area

4 CONCLUSION

In this study, we characterized the seasonal variation of sampling errors in the Han River Basin using the WGR model. The characterization of sampling errors was done for each month and also for the downstream plain area and the upstream mountain area, separately. As results of the study we conclude:

(1) The pattern of sampling errors estimated are obviously different from the seasonal pattern of monthly rainfall amounts. This result may be understood from the fact that the sampling error is estimated not simply by considering the rainfall amounts, but by considering all the mechanisms controlling the rainfall propagation along with its generation and decay. As the major mechanism of moisture source to the Korean Peninsula is obviously different each month, it seems rather normal to provide different pattern of sampling errors from that of monthly rainfall amounts.

(2) The sampling errors estimated for the upstream mountain area is about twice higher than those for the down stream plain area. It is believed to be because of the higher variability of rainfall in the upstream mountain area than in the down stream plain area. This has also been revealed in the parameters estimated. That is, the number of storms in the upstream mountain area was estimated significantly higher than that in the downstream plain area, but the cell intensity a little lower. Thus, more frequent but less intense storms in the mountain area can be expected due to the orographic effect, but the total amount of rainfall in a given period still remains almost the same.

Acknowledgements
This research was supported by Korea Research Foundation grant (KRF-99-041). All contributions are gratefully acknowledged.

REFERENCES

Graves, C. E., Valdes, J. B., Shen, S. S. P. and North, G. R. (1993). Evaluation of Sampling Errors of Rainfall from Space-borne and Ground Sensors, *J. of Appl. Meteorol.*, 32, 374-384.

Gupta, V. K. and Waymire, E. (1987). On Taylor's Hypothesis and Dissipation in Rainfall, *J. Geophys. Res.*, 92, 9657-9660.

Ha, E. and G. R. North, Use of Multiple Gauges and Microwave Attenuation of Precipitation for Satellite Verification, J. of Atmos. and Ocean. Tech., 11(3), 629-636, 1994.

Islam, S., Bras, R. L. and Rodriguez-Iturbe, I. (1988). Multi-dimensional Modeling of Cumulative Rainfall: Parameter Estimation and Model Adequacy through a Continuum of Scales, *Water Resour. Res.*, 24, 992-995.

Jung, K., Yoo, C. and Kim, J.-H. (2000). Genetic Algorithm Application for a Multi-dimensional Precipitation Modep Parameter Estimation, submitted, *Journal of Korea Water Resources Association*, 2000.

Koepsell, R. W. and Valdes, J. B. (1991). Multi-dimensional Rainfall Parameter Estimation from Sparse Network, *ASCE J. Hydraulic Eng.*, 117, 832-850.

Korea Meteorological Administration (1995). *Monthly Meteorological Summary*, Korea Meteorological Administration.

North, G. R. and Nakamoto, S. (1989). Formalism for Comparing Rain Estimation Designs, *J. Atmos. Ocean. Tech.*, 6, 985-992.

North, G. R., Shen, S. S. P., and Upson, R. B. (1991). Combining Rain Gages With Satellite Measurements for Optimal Estimates of Area-Time Averaged Rain Rates, *Water Resour. Res.*, 27, 2785-2790.

North, G. R., Valdes, J. B., Ha, E., Shen, S. S. P. (1994). The Ground-Truth Problem for Satellite Estimates of Rainfall, *J. Atmos. Ocean. Tech.*, 11(4), 1035-1041.

Valdes, J. B., Nakamoto, S., Shen, S. S. P., and North, G. R. (1990). Estimation of Multi-dimensional Rainfall Parameters by Areal Estimates of Oceanic Rainfall, *J. Geophys. Res.(Atmos.)*, 95(D3), 2101-2111.

Valdes, J. B., Ha, E. Yoo, C. and North, G. R. (1994). Stochastic Characterization of Space-Time Rainfall: Implications for Remote Sensing, *Advances in Water Resources*, 17, 47-99.

Waymire, E., Gupta, V. K. and Rodriguez-Iturbe, I. (1984). Spectral Theory of Rainfall Intensity at the Meso-beta Scale, *Water Resour. Res.*, 20(10), 1453-1465.

Yoo, C. (2000). On the Sampling Errors from Raingauges and Microwave Attenuation Measurements, *Stochastic Environmental Research and Risk Assessment.* 14(1), 69-77.

Yoo, C., Valdes, J. B. and North, G. R. (1996). Stochastic Modeling of Multi-Dimensional Rainfall Fields Considering Spectral Structure, *Water Resour. Res.*, 32(7), 2175-2187.

Table 1. Summary of typical parameters of the WGR model and their example estimates

Parameter	Description	Order of Magnitude	Estimates (GATE)
λ_m	rain band arrival rate	bands/hour	0.0128
ρ_L	mean density of cluster potential	clusters \km^2	0.0038
$<\upsilon>$	mean number of cells per cluster		3.82
β	cellular birth rate	cells/hour	0.355
σ	cell location parameter within a cluster potential region	km	10.0
α^{-1}	mean cell age	hour	0.58
D	spatial range of cell intensity	km	3.0
i_0	raincell intensity at cell center at the time of birth	mm/hour	55.06
$\|U_b\|$	rainband speed relative to the ground	km/hour	10.0
$\|U_c\|$	cell speed relative to the band	km/hour	0.0

Table 2. Parameters estimated for the downstream plain area and for the upstream mountain area

Month	Region	λ_m	β	$<\upsilon>$	α	ρ_L	i_0
May	Plain	0.0107	1.0000	10.9991	3.3922	0.0020	50.0053
	Mountain	0.0144	1.0040	10.9494	4.2814	0.0020	68.9469
June	Plain	0.0100	1.0000	9.7543	3.8924	0.0020	92.1858
	Mountain	0.0131	1.0746	19.8374	3.7334	0.0017	72.0468
July	Plain	0.0237	1.0003	19.6915	3.9522	0.0020	52.4183
	Mountain	0.0326	1.0000	19.9995	4.0099	0.0020	68.2346
August	Plain	0.0151	1.4345	19.8945	3.1239	0.0019	64.2190
	Mountain	0.0209	1.4831	19.9517	3.4790	0.0018	106.2786
September	Plain	0.0100	1.0000	18.5454	3.1023	0.0020	50.0000
	Mountain	0.0100	1.0000	17.5801	3.1000	0.0020	50.0000
October	Plain	0.0100	1.2510	6.4654	3.2463	0.0019	63.8575
	Mountain	0.0100	1.0000	6.4522	4.2868	0.0018	50.0080

Table 3. Comparison of basic statistics derived and observed in the downstream plain area

Month		1hr-mean	1hr-var	1hr-corr	6hr-var	6hr-corr	Ccorr
May	Observed	0.121	0.89	0.493	11.864	0.409	0.360
	Model	0.115	0.924	0.559	11.778	0.083	0.275
June	Observed	0.190	1.664	0.500	27.130	0.312	0.450
	Model	0.196	1.576	0.565	27.911	0.307	0.375
July	Observed	0.446	5.830	0.451	86.877	0.328	0.300
	Model	0.445	6.727	0.551	67.751	0.183	0.183
August	Observed	0.376	4.799	0.471	81.736	0.323	0.300
	Model	0.357	5.376	0.448	64.860	0.232	0.295
September	Observed	0.224	2.541	0.548	53.222	0.405	0.510
	Model	0.216	3.175	0.442	37.779	0.082	0.334
October	Observed	0.038	0.382	0.318	3.003	0.165	0.130
	Model	0.045	0.352	0.249	2.836	0.165	0.114

* Var : Variance; Corr : Correlation; Ccorr : Crosscorrelation (50km)

Table 4. Comparison of basic statistics derived and observed in the upstream mountain area

Month		1-mean	1-var	1-corr	6-var	6-corr	Ccorr
May	Observed	0.111	0.820	0.416	12.075	0.337	0.150
	Model	0.114	0.841	0.428	11.608	0.304	0.108
June	Observed	0.200	3.266	0.367	35.424	0.265	0.170
	Model	0.208	3.208	0.297	34.183	0.135	0.168
July	Observed	0.397	4.208	0.482	74.355	0.354	0.150
	Model	0.402	4.855	0.391	52.891	0.070	0.143
August	Observed	0.326	4.693	0.395	58.756	0.291	0.120
	Model	0.318	5.202	0.429	53.184	0.228	0.105
September	Observed	0.232	2.207	0.510	42.687	0.392	0.350
	Model	0.188	2.802	0.422	32.165	0.077	0.288
October	Observed	0.025	0.078	0.334	0.977	0.185	0.090
	Model	0.022	0.100	0.327	0.918	0.054	0.049

* Var : Variance; Corr : Correlation; Ccorr : Crosscorrelation (50km)